COMPARING THE WEATHERING ENVIRONMENT OF PERMIAN AND MODERN ANTARCTIC PROGLACIAL LAKE SEDIMENTS: MINERALOGICAL AND GEOCHEMICAL STUDY

Undergraduate Research Thesis
Submitted in partial fulfillment of the requirements for graduation
with research distinction in Earth Sciences
in the undergraduate colleges of
The Ohio State University

By

Shelby A. Brewster
The Ohio State University
2017

Approved by

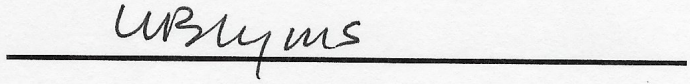

Dr. W. Berry Lyons, Project Advisor
School of Earth Sciences

Table of Contents.

Abstract.

The Antarctic continent has been in a polar to subpolar position since the Permian period. Although it has experienced milder climates over this time period as evidenced by corals in the fossil record, Antarctica did undergo extensive glaciation during the Permian. This is based on the abundance of Permian tillites (sedimentary rocks derived from glacier tills) found in the Transantarctic Mountains. In this research, I have compared Permian age proglacial lake sediments that are associated with tilites to modern proglacial lake siltstones and mudstones from Antarctica. This was done to determine the climate, especially the amount of glacier melt that occurred when these Permian sediments were deposited. The modern lake sediments are deposited in perennially ice-covered lakes by ephemeral streams that only flow 6 to 12 weeks a year. The geochemical analyses of the Permian samples and the modern sediments from Lake Hoare in the McMurdo Dry Valleys suggest that the Permian samples are more highly chemically weathered than the modern sediments. The mineralogy of Lake Hoare sediments contain more primary minerals than chemical weathering produced minerals in the Pagoda Formation rocks, thus supporting the geochemical analysis that the Pagoda Formation minerals have been more weathered. All these data suggest that the Permian lake samples were deposited in a warmer, more hydrogeologically active environment than were the modern lake sediments. These data support previously published sedimentological and paleontological data that the Pagoda samples were deposited under more temperate or warm-based proglacial conditions than what is observed in the McMurdo Dry Valleys today.

ACKNOWLEDGEMENTS.

I wholeheartedly thank everyone in the Lyons research group who selflessly offered their time and guidance throughout the process of the analysis and writing of my thesis. My advisor, Dr. Berry Lyons, was extremely encouraging and helped me maintain a positive attitude and strive towards maximizing my productivity. I would like especially acknowledge Dr. Sue Welch; she was the logistical backbone to my success, having provided me with the essential resources and connections that allowed the thesis writing process to run smoothly. I would also like to thank Dr. Julie Sheets, Kathy Welch, Dr. Chris Gardner, Melisa Diaz, Sydney Olund, Sam Israel, and Elsa Saelens for their valuable advice and support every step of the way.

The Byrd Polar and Climate Research Center makes it possible for undergraduate students such as me and other scientists alike to access thousands of samples that allow us to contribute to the understanding of our earth and its natural processes. I would like to thank the entire staff of the Polar Rock Repository for their commitment to the scientific community and helping facilitate the ease of transferring scientific samples for research purposes. I would like to thank Dr. Anne Grunow, senior research scientist and curator of the Polar Rock Repository, for providing me with the rock samples I analyzed for my research as well as Dr. Peter Doran of LSU for providing the Lake Hoare sediments to the Lyons research group.

Colleagues and friends are among the most underrated aspects of personal growth and achievement of an individual. I want to express my genuine gratitude and appreciation of my School of Earth Sciences classmates. I attribute being surrounded by such intelligent, competitive, and adventurous people to my academic and personal success. I would like to especially acknowledge George Domer, Taylor Hollis, Ben Holt, Scott Hull, Brandi Lenz, Bryan O'Reilly, Nick Rodgers, and Judith Straathof for helping shape me into the person and scientist

that I have become. Our late-night study sessions, mutual commiserations over classwork, SES van adventures, and grueling hours spent together in the hot Utah sun are cherished memories that I will always hold near to my heart.

Finally, I would like to thank the people who are the foundation of my life: my family. Both of my parents grew up in financially struggling households and neither had the opportunity to attend college fulltime. Having worked so hard their whole lives to provide the best life for their daughters, they realized the importance of encouraging and furthering our education. Thank you for supporting and encouraging me no matter how silly or unrealistic my aspirations may have been.

List of Figures.

List of Tables.

1. Introduction.

Antarctica has been situated in a polar to subpolar position from the Paleozoic time period to the present. During the late Paleozoic, Antarctica was located within the Gondwana supercontinent adjacent to South America, Africa, India, and Australia. The climatic conditions resulting from the continent's polar path during the late Paleozoic subjected it to an extensive glaciation period, spanning from the late Carboniferous to the early Permian (Lopez-Gamundi and Buatois, 2010). In this study, two sets of Antarctic lacustrine samples from different times and locations (described under geologic setting) were analyzed. These lacustrine samples come from the Central Transantarctic Mountains (CTAM): Permian siltstones and mudstones (Pagoda samples) and modern Lake Hoare proglacial lake sediments (LH sediments) from Taylor Valley within the McMurdo Dry Valleys (MDV). The Pagoda samples are from the Permian-Carboniferous Pagoda Formation within the Beacon Supergroup and they record evidence of the late Paleozoic glaciation (Lopez-Gamundi and Buatois, 2010). Lopez-Gamundi and Buatois (2010) created a reconstruction of this time period (Figure 1), categorizing three different glacial episodes to help visualize the changing paleoclimate concurrently with Gondwana's paleo-migration.

Figure 1. Gondwana during the Late Paleozoic with categorized glacial episodes and the general trend of eastward movement across the pole (Lopez-Gamundi and Buatois, 2010).

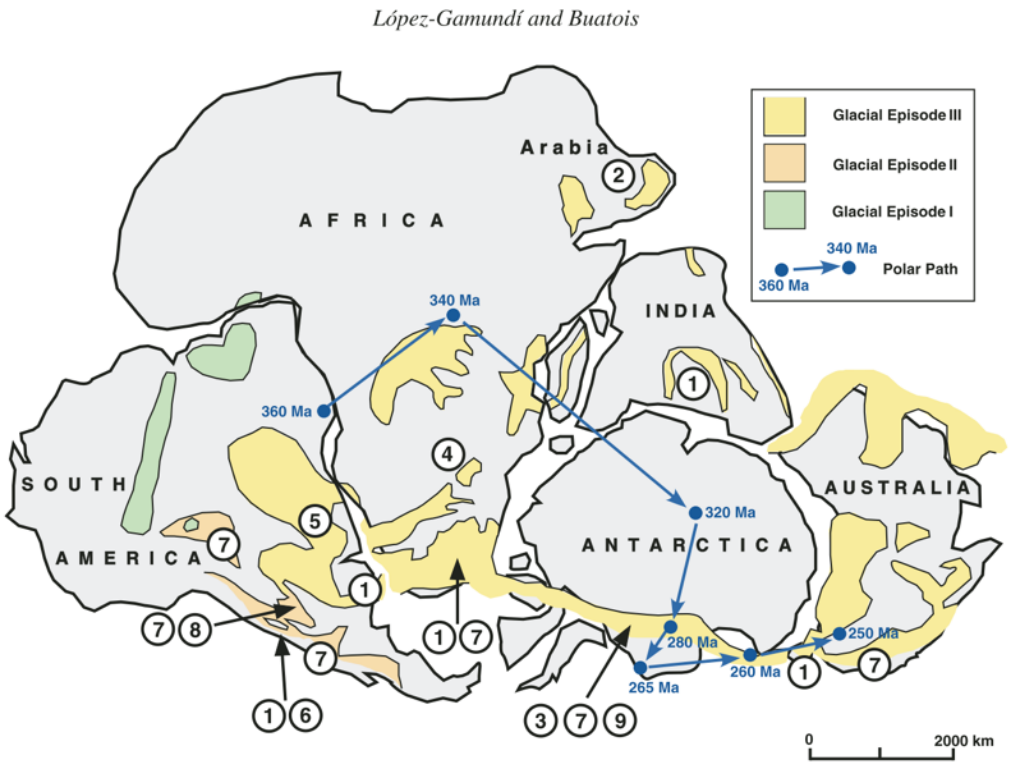

Dr. John F. Lindsay (1970) of the Ohio State University intensively studied and described the lithology, paleo-ice flow structures, and the paleogeography of the Permian Pagoda Formation and its younger, overlying units. The Victoria Group strata in the CTAM begins with the lowermost unit of the Pagoda Formation defined by glacial tillites deposited disconformably on massive Devonian to Proterozoic quartzose sandstone (Lindsay 1970). The uppermost units of the Pagoda Formation mark the onset of rising temperatures with glacial tillites transitioning to the overlying Mackellar Formation's (figure 2) thinly bedded shales and sandstones (Lindsay 1970). Lithology of the successive formations within the Victoria Group continue to reflect post-

glacial environments such as alluvial planes, shallow bodies of water, and high energy streams (Faure and Mensing, 2010).

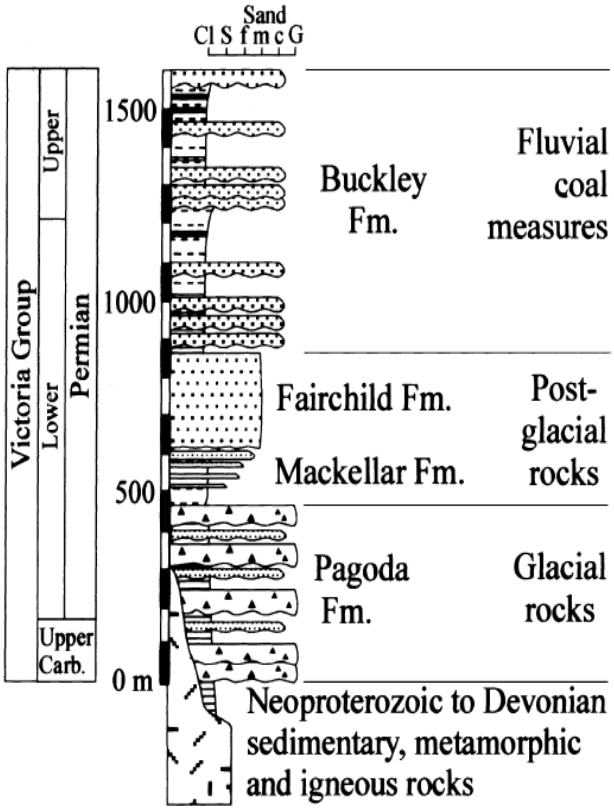

Figure 2.

Late Carboniferous to Permian units of the Victoria Group and a simplified depiction of their lithology. The figure illustrates the progression towards a warmer climate from the Lower to Upper Permian period (Isbell et al., 2001).

The MDV where the modern Lake Hoare sediments were collected is at 78° S latitude and are the largest ice-free area of Antarctica. There has been little to no bulk geochemistry and little mineralogical analysis of the Lake Hoare sediments until now.

2. Geologic Setting.

2.1 Mt. Butters.

The Pagoda Formation throughout the CTAM is composed of massive glacial tillites, sandstones, and mudstones accumulated from the varying depositional environments created by the transgression and regression of Paleozoic ice sheets. The Mt. Butters region near Shackleton Glacier reveals an outcrop of basal fine-grained Pagoda Formation that was deposited non-conformably on an Ordovician granite surface (Figure 3) (Isbell et al., 2001). The presence of basal diamictites interbedded with successions of coarsening upward siltstone suggests an aqueous depositional environment "by suspension settling, rain out of ice-rafted debris, and deltaic progradation" (Isbell et al, 2001, p. 953). The succession of fine-grained sediments to overlying massive diamictite (Figure 4a) supports the interpretation of a frequently changing dynamic environment recorded as proglacial lakes being covered by transgressive Paleozoic ice sheets (Isbell et al., 2001). The notable preservation of glacigenic sedimentation onset suggested by the fine-grained basal materials at Mt. Butters appears to have been possible due to deposition on the lee side of a previous granite buttress, preventing erosion of the basal Pagoda sediments by transgressing glacial ice (Isbell et al., 2001).

Figure 3. Exposed Permian units overlapping granite basement, Basal Pagoda Formation thickening towards east-northeast (Isbell et al., 2001).

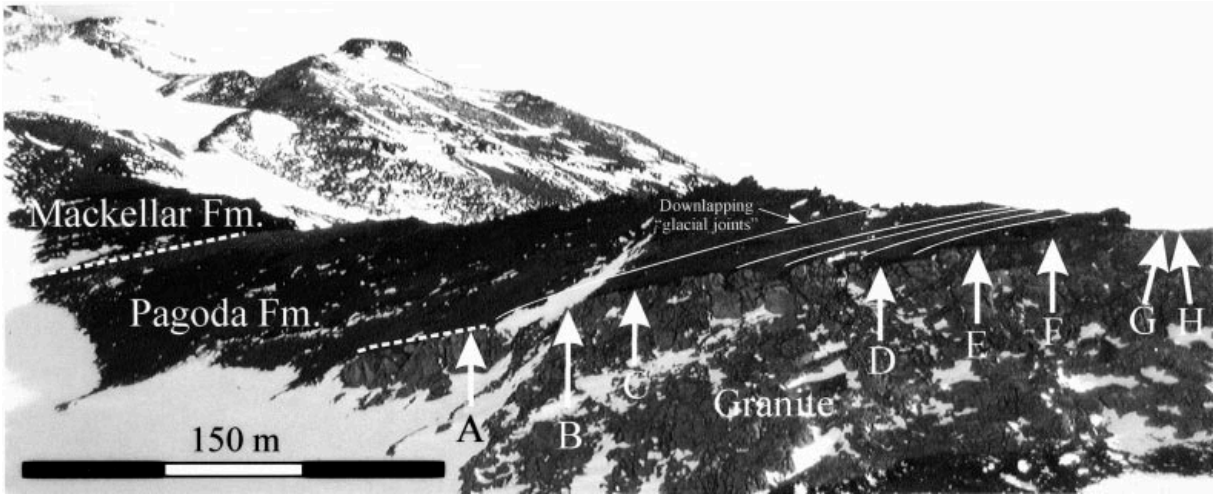

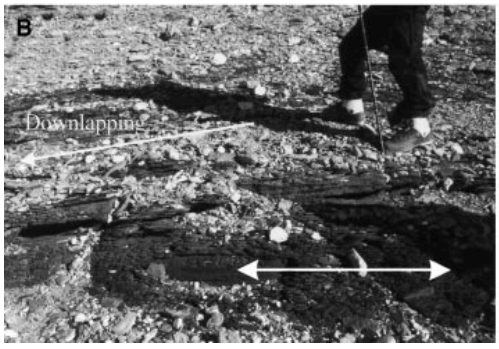

Figure 4.

A). Shows complete siltstone to sandstone succession.

B). Fine-grained sandstone sloping down on top of underlying siltstone.

C). Symmetrical ripples occurring on uppermost sandstone layer with each sandstone-siltstone succession; ripples provide evidence of a lacustrine environment (Isbell et al., 2001).

2.2 Lake Hoare.

The McMurdo Dry Valleys located in southern Victoria Land are the largest ice-free areas in Antarctica and are considered polar deserts with a mean annual temperature of -20° and around 3 centimeters of annual rainfall (Doran et al., 2002; Fountain et al., 2010). A notable feature is the abundance of closed basin, perennial ice-covered lakes. Among these lakes is Lake Hoare in Taylor Valley, covering a surface area of 1.8km^2 with water sources supplied by direct glacial melt and runoff from ephemeral streams. It is the freshest of the Taylor Valley lakes (Lyons et al., 2000). Sediment covering the lake is sourced from both aeolian sediments melting through the ice-cover and fluvial transportation primarily from inflow from Anderson Creek in the NE corner of the lake and supraglacial melt from the Canada Glacier (Allen et al., 2015).

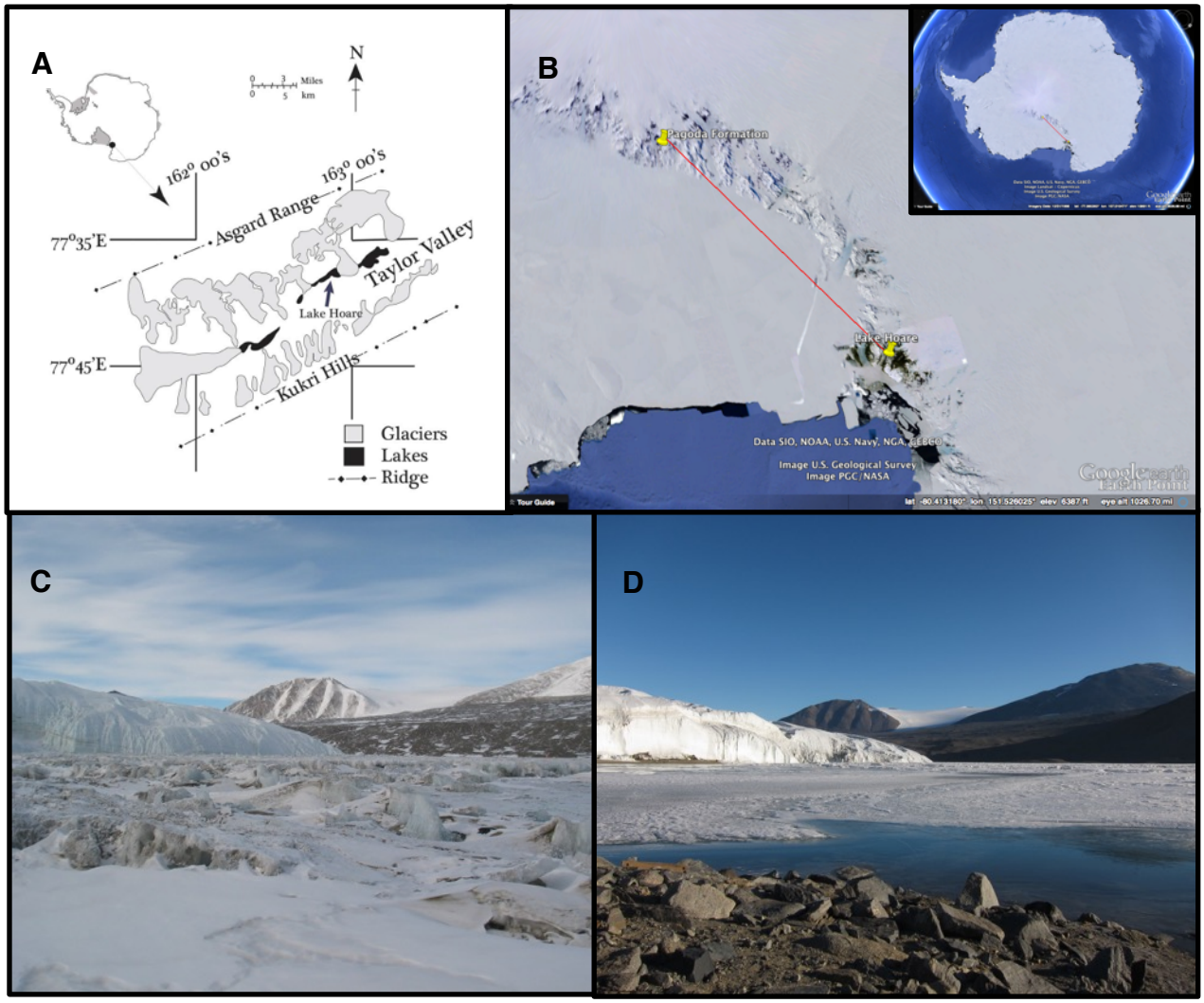

Figure 5. A). Relative position of Lake Hoare within Taylor Valley (Allen et al, 2015). B). Relative location of Lake Hoare to Mt. Butters. C). Ground photo (provided by Kathleen Welch, The Ohio State University) of Lake Hoare facing Canada Glacier taken in October. D). Same position as photo C taken in January.

3. Methods.

The Permian sedimentary rocks were collected by Dr. Molly Miller of Vanderbilt University in the CTAM, Victoria Land, Antarctica. Dr. Anne Grunow of the Polar Rock Repository at The Ohio State University provided the samples for analysis. The modern sediments from Lake Hoare in the MDV were collected via core sampling by Dr. Peter Doran of Louisiana State University (Doran et al., 2002). The top 16 centimeters of the core were analyzed for this study. The following methods were utilized for analysis of the Permian samples and modern lake sediments geochemical and mineralogical compositions: 1) mineralogy of the Permian samples via thin section analysis 2) X-ray Diffraction (XRD) 3) geochemistry via X-ray Fluorescence (XRF) and 4) Inductively Coupled Plasma-Atomic Emission Spectroscopy (ICP-AES) in both the Pagoda Formation samples and the Lake Hoare sediments. Geochemical results were used to interpret the extent of weathering via Chemical Index of Alteration (CIA) of Nesbitt and Young (1983) and also by a comparison of the trace element composition against normalized estimations of upper continental crust trace element composition using the method of Rudnick and Gao (2003). The thin sections were made by Spectrum Petrographics in Vancouver, Washington. The thin section and XRD analyses were done at Ohio State as was the XRF analysis of the Lake Hoare sediments. The geochemical analysis of the Pagoda samples was done by SGS Mineral Services, Ontario Canada.

3.1 Thin Section Analysis.

Four Pagoda siltstone and mudstones (table 1) made into thin sections were observed using a Leica DM750 P standard petrographic microscope to determine the 1) major minerals present 2) order of percent abundance 3) grain size 4) sorting and roundness of the minerals 5) matrix composition, accessory minerals, and the alteration of the minerals. Undulose extinction,

mineralogical alteration, bedding planes, optic sign, pleochroism, and birefringence were observed to determine the previously mentioned characteristics. Estimations of the provenance, degree of weathering, and depositional environment were made from the results of mineral compositions and weathering.

Sample Name	Notes	Field Location	Coordinates
Pagoda 1	Siltstone mid-upper Pagoda Lake	Mt. Butters	-84.963, -177.3
Pagoda 2	Siltstone lower Pagoda Lake	Mt. Butters	-84.963, -177.3
Pagoda 3	Mudstone on granite basement	Mt. Butters	-84.883, -177.5
Pagoda 4	Mudstone on granite basement	Mt. Butters	-84.883, -177.5

Table 1. Description of the four Pagoda samples chosen to be made into thin sections.

3.2 Powder X-ray Diffraction.

The Pagoda samples and Lake Hoare sediments were prepared for XRD analysis at the Subsurface Energy Characterization and Analysis Laboratory (SEMCAL) at Ohio State University School of Earth Sciences. The samples were crushed by hand into a fine powder using a corundum mortar and pestle, loaded into stainless steel sample holders, and analyzed with a PANanalytical X'pert Pro X-ray Diffractometer equipped with a high speed X'Celerator detector. X-rays were generated at a voltage of 45 keV 40 ma current, and a goniometer step size of 0.02 degrees 2θ as used. Constructive interference of X-rays scattered from electrons in the crystal structures of minerals occurs when Bragg's Law ($n\lambda=2d\sin\theta$) is satisfied. This allows calculation of an inter-planar spacing (d-spacing) corresponding to each measured 2θ reflection

angle for CuKα radiation (λ = 1.54 Å). PANanalytical Highscore Plus software and the PDF 4+ mineral database were used to match patterns of d-spacings in the database to experimental d-spacings to identify minerals in the samples.

3.3 Geochemical Analysis.

The geochemical analysis of the Pagoda Formation samples was done by SGS Mineral Services in Ontario, Canada. Samples were crushed and split into representative subsamples using a riffle splitter and then pulverized so that at least 85% of the mass was 75 micrometers or smaller. The major oxides were analyzed by X-ray fluorescence spectroscopy via borate fusion. The minor and trace elements were analyzed by the ICP-AES after sodium peroxide fusion and acid dissolution. The Lake Hoare sediments were crushed and analyzed for both major oxides and minor and trace elements in the School of Earth Sciences XRF facility in Mendenhall Lab after manual crushing to <150 micrometer sized particles. Samples were analyzed on pressed pellets with a polyvinyl alcohol binder using a Phillips PW 2450 XRF spectrometer. The Lake Hoare sediments analyzed at The Ohio State University were set to USGS standards AG V-1, BIR-1, G-2 and SDC-1 were measured within 12% of all reported values except Na_2O (49%), Cr (82%) and Ni (82%).

3.3.1 Spider Diagrams.

XRF data, major, minor, and trace elements were plotted in Microsoft Excel on a logarithmic scale in order of magmatic compatibility from continental crust elements to mantle elements from left to right. The four Pagoda samples and Lake Hoare sediments' elemental compositions in units of parts per million were divided by (i.e. "normalized to") the average upper continental crust compositions (Rudnick and Gao, 2003). The x-axis represents continental to mantle elemental compatibility from left to right while the y-axis represents elements above 1 as

enriched and depleted below 1 compared to upper continental crust. The idea behind this normalization is that the graphic should easily demonstrate the most whole elements lost during chemical weathering (values < 1), and the ones that are refracting or concentrated by the chemical weathering process (values > 1).

3.3.2 Chemical Index of Alteration.

The calculated CIA found in equation 1 proposed by Nesbitt and Young (1982) was used to estimate the degree of chemical weathering by quantifying the proportion of both Pagoda and Lake Hoare sediments' aluminum oxide weight percentages against alkali earth and metal concentrations. During chemical alteration, soluble elements such as calcium, sodium, and potassium are some of the most mobile elements and hence are the first to be removed from the rocks. Therefore, the CIA increases as the degree of chemical weathering increases as these mobile elements are solubilized. A high CIA implies the preferential removal of calcium, sodium, and potassium relative to the immobile aluminum, whereas a low CIA represents minimal chemical weathering, conditions common in cold, arid climates. Fresh basalts and granites have values of 30-45 and 45-50, respectively while values from clay minerals produced by weathering range from 75-100 (Nesbitt and Young, 1982).

Equation 1). $CIA = [Al_2O_3 / (Al_2O_3 + CaO + Na_2O + K_2O)] \times 100\ \%$

4. Results.

4.1 Thin Section Analysis of Pagoda Samples.

The two siltstones and two mudstones contain clasts of sub-angular to sub-rounded quartz and feldspar, clinochlore, muscovite, and accessory zircon. The shapes of the clasts indicate minimal mechanical weathering as most of the clasts have retained their original shapes. There is evidence of extensive alteration of oxide minerals and abundant fine-grained clays and phyllosilicates that indicate a high degree of chemical weathering. The compositions of the clays are impossible to determine through petrographic analysis. The mineral assemblage of quartz, feldspar, and phyllosilicates indicates a granititic provenance (Lindsay 1970).

4.1.1 Siltstone Clasts.

Feldspar. Clasts are sub-angular to sub-rounded and moderately sorted up to 0.02mm. Most of the clasts display undulose extinction and are primarily unaltered. The evidence of clasts that have been altered into clay are as seen in Figure 6l. Feldspar makes up approximately 50% of the thin section.

Quartz. Clasts are sub-angular to sub-rounded with an average length of 0.025mm (Figure 6a). The siltstones contain a few clasts that are up to 0.3mm in length. Many of the clasts exhibit strain with undulose extinction. Quartz makes up approximately 33% of the thin section.

Clinochlore. The phyllosilicates are non-crystalline with a mesh-like texture. There are few remaining laths; those remaining are up to 0.1mm in length. The colors appear distinctly green (Figure 6k) in plane polarized light (PPL) with anomalous dark blue interference colors in cross polarized light (XPL); dark blue interference colors are a diagnostic optical characteristic of chlorite's magnesium end-member, clinochlore (Figure 6m). The clasts occur within altered quartz and feldspar grains and around their borders. What appear to be muscovite laths with up

to 3rd order birefringence in XPL commonly display a border of anomalous blue interference colors (Figure 6m). This is interpreted to be chloritization of muscovite to clinochlore. Clinochlore makes up approximately 9% of the thin section.

Clays. Very fine grained, indistinguishable clays displaying up to 2rd order birefringence. Clays make up approximately 8% of the thin section.

4.1.2 Mudstone Clasts.

Clays. Clays are fine grained and display up to 3rd order birefringence. Colors appear brown in PPL and dark brown in XPL with some hints of high birefringence (Figure 6b). The clays are weathering products of quartz, feldspar, and phyllosilicates. Clays make up approximately 75% of the section.

Feldspar. Clasts are sub-angular to sub-rounded and poorly sorted with an average length of 0.02mm. All the clasts display undulose extinction. Many feldspars in the mudstones have been completely altered and replaced by clays, leaving behind angular, square outlines of former clasts in the matrix (Figure 6b). Some of the remaining clasts are relict (Figure 6e). Feldspar makes up approximately 14% of the thin section.

Quartz. Clasts are sub-angular to sub-rounded with an average length of 0.025mm (Figure 6f) with a few clasts up to 0.3mm in length. Most clasts exhibit strain with undulose extinction (Figure 6d) and show alteration to phyllosilicates like clinochlore (Figure 6j). Quartz makes up approximately 6% of the thin section.

Clinochlore. Alteration product displaying mesh-like texture. Distinct green color in PPL and anomalous blue interference colors. Mostly occurs within quartz and feldspar grains (Figure 6j). Clinochlore makes up approximately 4% of the thin section.

Biotite. The biotite laths are an accessory mineral with an average length of 0.02mm. They occur in scattered laths throughout thin sections and display diagnostic brown pleochroism in PPL (Figure 6i) and up to 2rd order birefringence. Biotite makes up approximately 1% of the thin section.

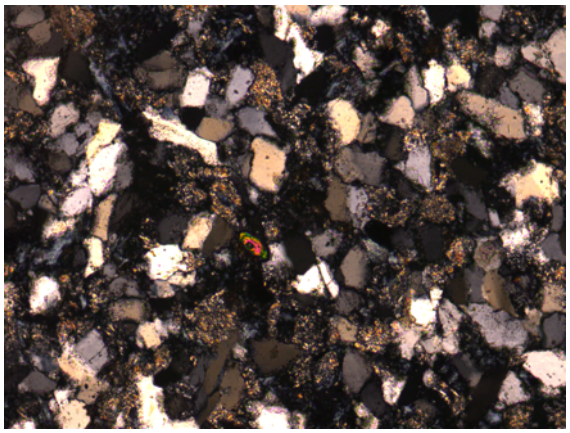

Figure 6a. Siltstone XPL (100x) angular quartz, feldspar, and zircon inclusion.

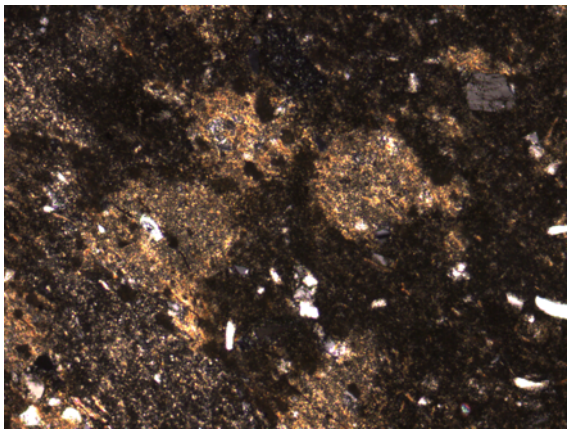

Figure 6b. Mudstone XPL (40x) broken quartz and remnants of feldspar replaced with clays (light brown shapes).

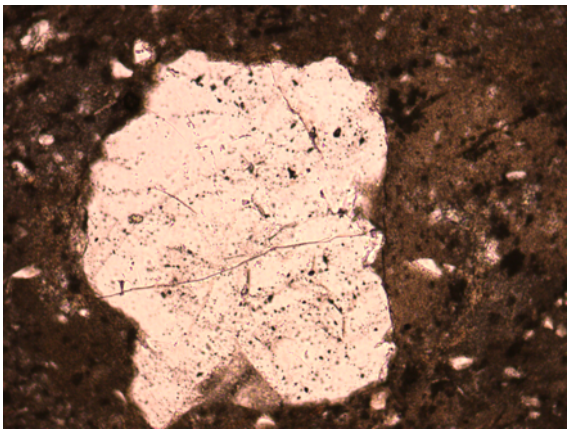

Figure 6c. Mudstone PPL (100x) quartz clast 0.35mm.

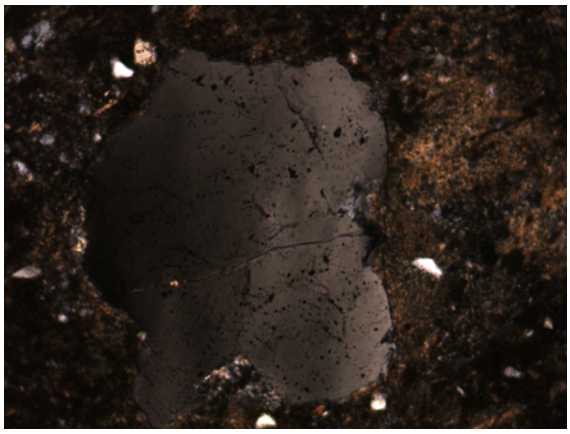

Figure 6d. Mudstone XPL (100x) quartz clast with undulose extinction.

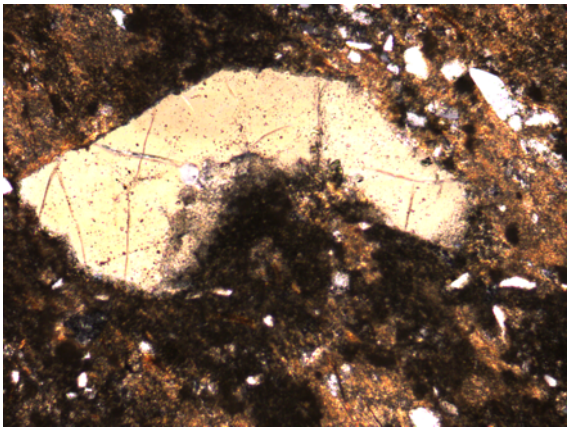

Figure 6e. Mudstone PPL (100x) relict angular feldspar clast.

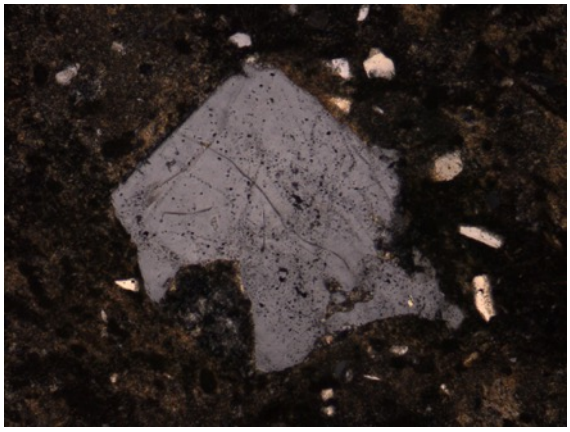

Figure 6f. Mudstone XPL (100x) quartz clast being altered to clinochlore.

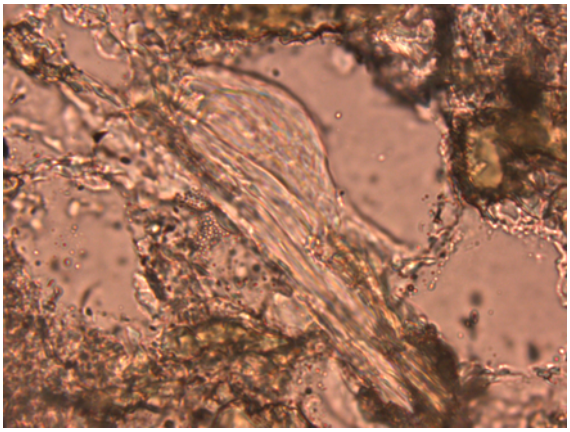

Figure 6g. Siltstone PPL (1000x) green phyllosilicate.

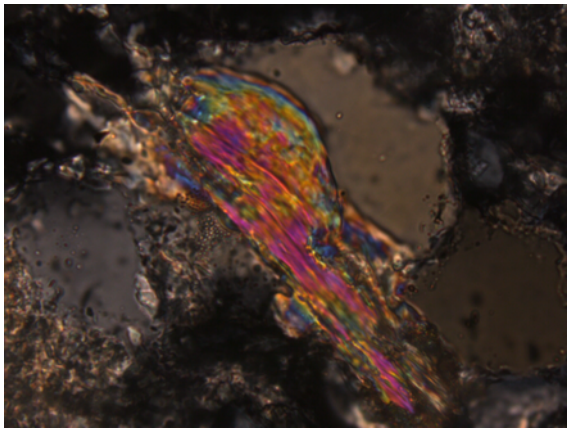

Figure 6h. Siltstone XPL (1000x) phyllosilicate with 3rd order birefringence.

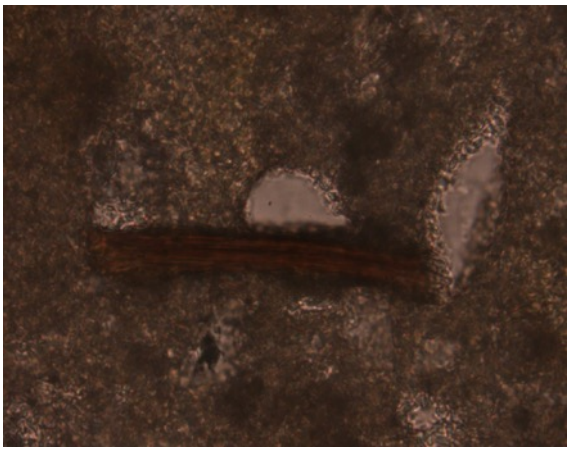

Figure 6i. Mudstone PPL (1000x) biotite lath displaying brown pleochroism.

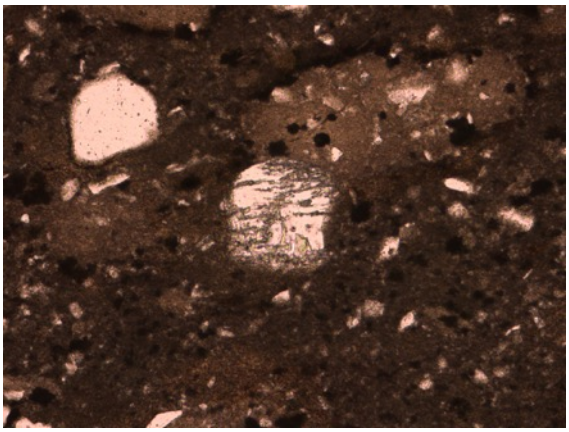

Figure 6j. Mudstone PPL (100x) quartz clast with clinochlore alteration.

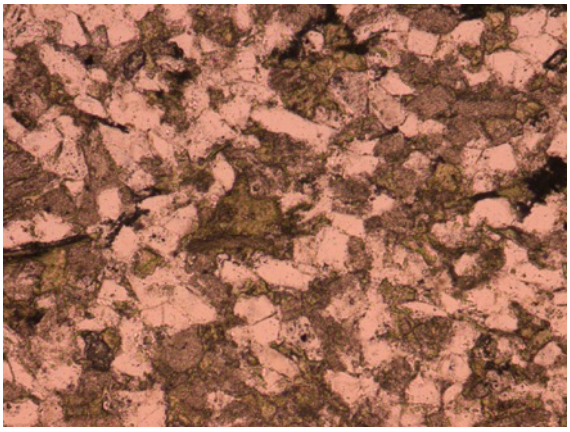

Figure 6k. Siltstone PPL (100x) clinochlore displaying distinct green colors.

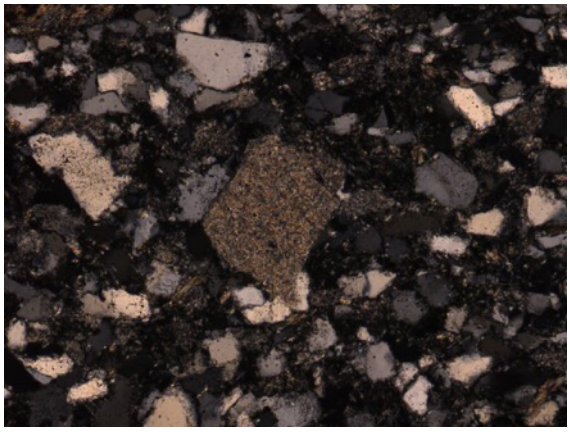

Figure 6l. Siltstone XPL (100x) feldspar grain altered into clay

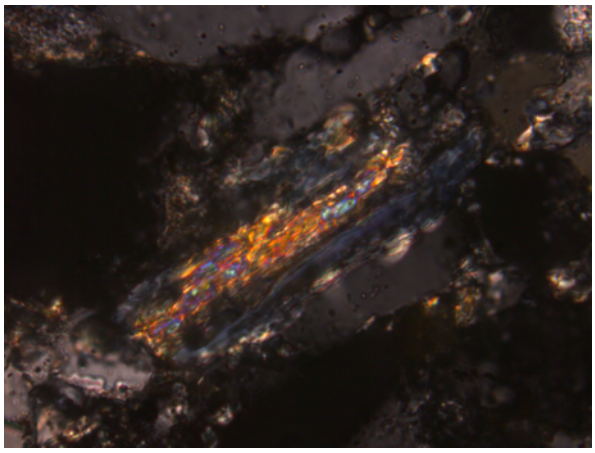

Figure 6m. Siltstone PPL (1000x) clinochlore displaying distinct green colors.

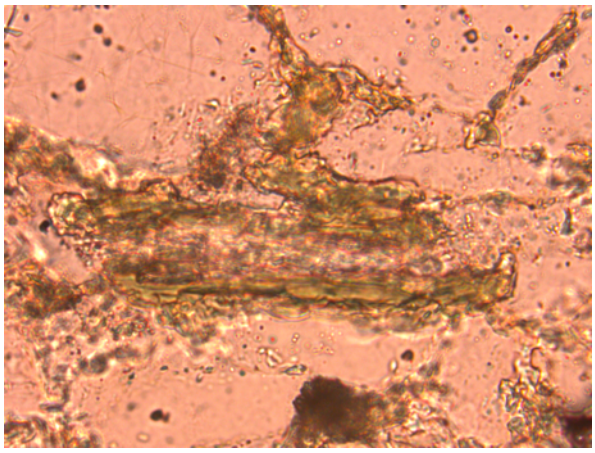

Figure 6n. Siltstone (1000x) muscovite being altered to clinochlore.

4.2 Mineralogy from XRD Analysis of Pagoda Samples and LH Sediments.

XRD revealed mineralogical differences that coincide with a greater amount of weathering in the Pagoda samples versus Lake Hoare sediments. Like the thin sections, the Pagoda samples reflect a granitic provenance with abundances of quartz, K-feldspar, and mica whereas Lake Hoare sediments indicate more mafic origins. Further sample preparation is needed to distinguish between clay compositions, particularly between illite, smectite, and kaolinite.

4.2.1 Pagoda Samples.

The asymmetric peak patterns observed in Figure 7 were interpreted to reflect low crystallographic symmetry minerals such as phyllosilicates and clays. The overlapping peaks of all three Permian samples, PRR1 and PRR3 (mudstones) are more similar compared to PRR2 (siltstone). PRR2 displays more symmetrical quartz peaks which is consistent with its siltstone lithology. All three contain low symmetry clay minerals which are common by-products of chemical weathering. Feldspar peaks were interpreted to be albite and potassium-bearing orthoclase and microcline. 14 Å peaks point towards a magnesium-rich phyllosilicate interpreted to be clinochlore (magnesium rich chlorite). Peaks associated with micaceous minerals were inferred to be muscovite, due to the granitic origins of the rocks. Exact composition of clays is not clearly identifiable and would require further detailed investigation. It is difficult to differentiate between muscovite and illite because both share the 10 Å d-spacings.

4.2.2 Lake Hoare Sediments.

The mineralogy (Table 2) of the Lake Hoare sediments is consistent throughout the 16 analyzed centimeters of sediments (Figure 8) of overlapping peak trends. The sharp, symmetric peaks indicate high-ordered minerals such as quartz and feldspar.

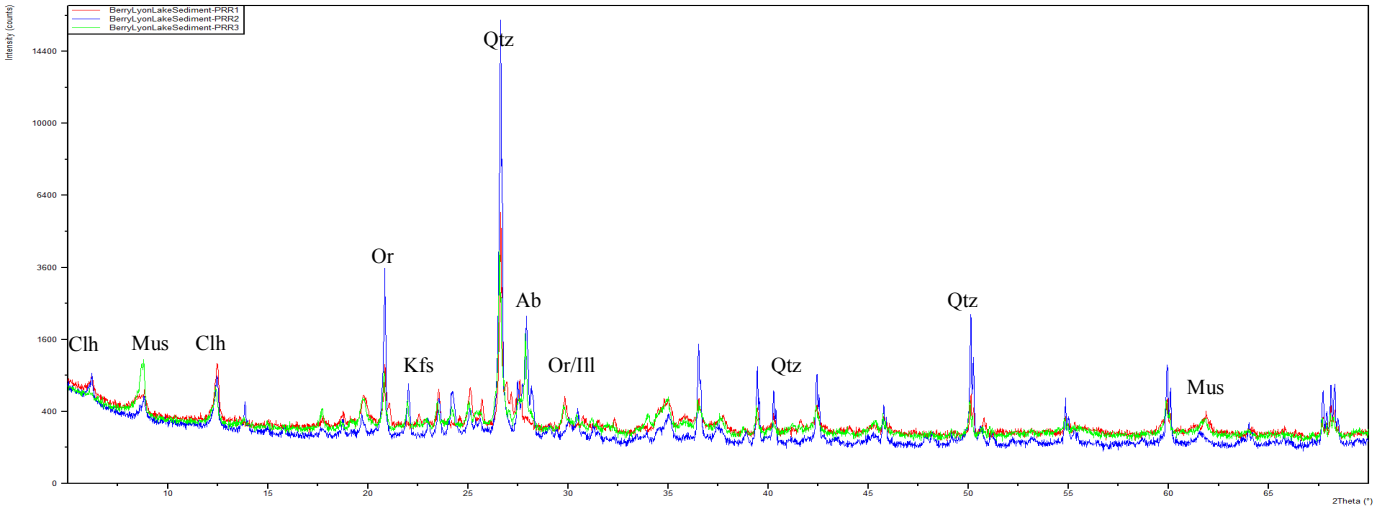

Figure 7. XRD patterns of Pagoda samples denoted as PRR1, PRR2, and PRR3.

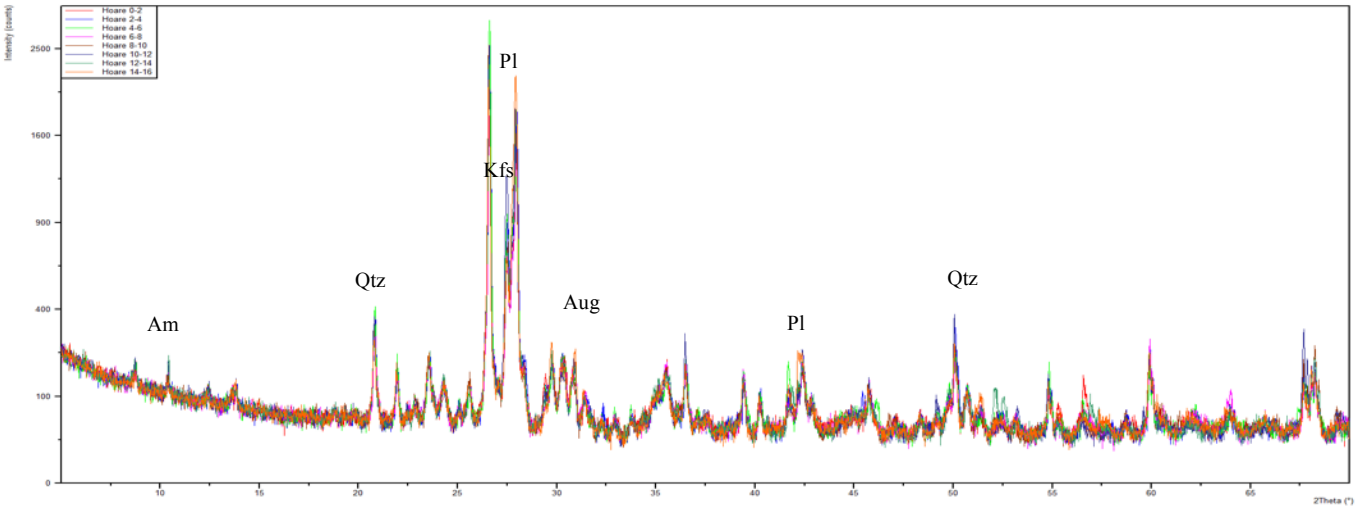

Figure 8. XRD patterns of all 16 cm of Lake Hoare sediments.

Sample Name	Mineralogy by XRD	Thin Section Mineralogy
Pagoda 1	Quartz, K-feldspar, muscovite, clinochlore, illite/smectite/kaolinite*	Illite/smectite/kaolinite*, feldspar, quartz, clinochlore, biotite
Pagoda 2	Quartz, albite, muscovite, clinochlore, illite/smectite/kaolinite*	Feldspar, quartz, clinochlore, illite/smectite/kaolinite*
Pagoda 3	Quartz, albite, muscovite, clinochlore, illite/smectite/kaolinite*	Illite/smectite/kaolinite*, feldspar, quartz, clinochlore, biotite
Lake Hoare	Quartz, plagioclase, K-feldspar, augite, enstatite, amphibole, biotite	**No thin sections**

Table 2.: Mineralogy of Pagoda and Lake Hoare samples determined through XRD analysis.

*-Additional sample preparation required to distinguish between clay compositions.

4.3 Geochemistry from XRF Analysis.

4.3.1 CIA Results.

The chemical index of alteration results for the Pagoda samples and Lake Hoare sediments suggest a different history of chemical weathering indicating different environments of deposition. The four Pagoda samples have CIA results greater than 66%, indicating that minerals in these rocks have undergone relatively high degrees of chemical weathering. On the other hand, the Lake Hoare values are much lower ranging from ~54% to ~55% (Table 4). The major oxide data from the Pagoda samples and Lake Hoare sediments are seen in Table 3. The CIA determinations based on the data in Table 3 are shown in Table 4.

Major Oxide (%)	Al_2O_3	CaO	Na_2O	K_2O
Pagoda 1	12.7	0.89	1.02	3.03
Pagoda 2	12	0.79	2.10	3.26
Pagoda 3	19.4	1.72	0.61	6.1
Pagoda 4	19.2	0.59	0.56	6.2
LH 14-16	13.7	5.80	3.05	2.39
LH 10-12	13.3	5.78	2.85	2.31
LH 6-8	13.1	6.07	2.79	2.20
LH 2-4	13.9	6.39	2.71	2.32
LH 0-2	14.1	7.00	2.68	2.45

Table 3. Major oxide compositions by weight percent of Pagoda samples and Lake Hoare sediments.

CIA Percentages									
Sample Name	Pagoda 1	Pagoda 2	Pagoda 3	Pagoda 4	LH 14-16	LH 10-12	LH 6-8	LH 2-4	LH 0-2
%	72%	66.1%	69.7%	72.3%	54.9%	54.8%	54.3%	54.9%	53.8%

Table 4. Calculated CIA results of Pagoda samples and Lake Hoare sediments.

4.3.2 Spider Diagrams.

The spider diagrams of major, minor, and trace elements for the Pagoda samples (Figure 9) reveal significant depletion in calcium and sodium concentrations in all 4 samples. The Lake Hoare sediments are only slightly depleted in sodium and are actually enriched in Calcium (Figure 10). Interestingly, all the Lake Hoare sediments (0-16cm) show very similar patterns, while there are larger differences in the patterns among the Pagoda samples.

.

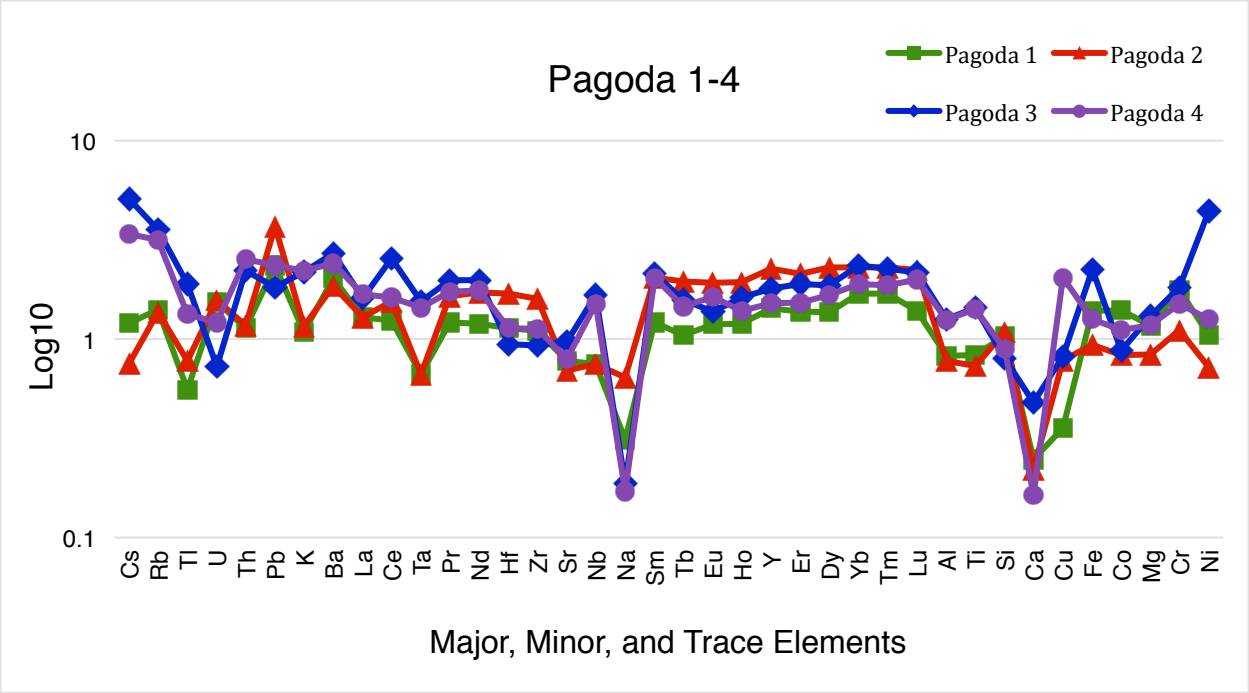

Figure 9. Spider diagram of major, minor, and trace elements of Pagoda samples in order of crustal compatibility.

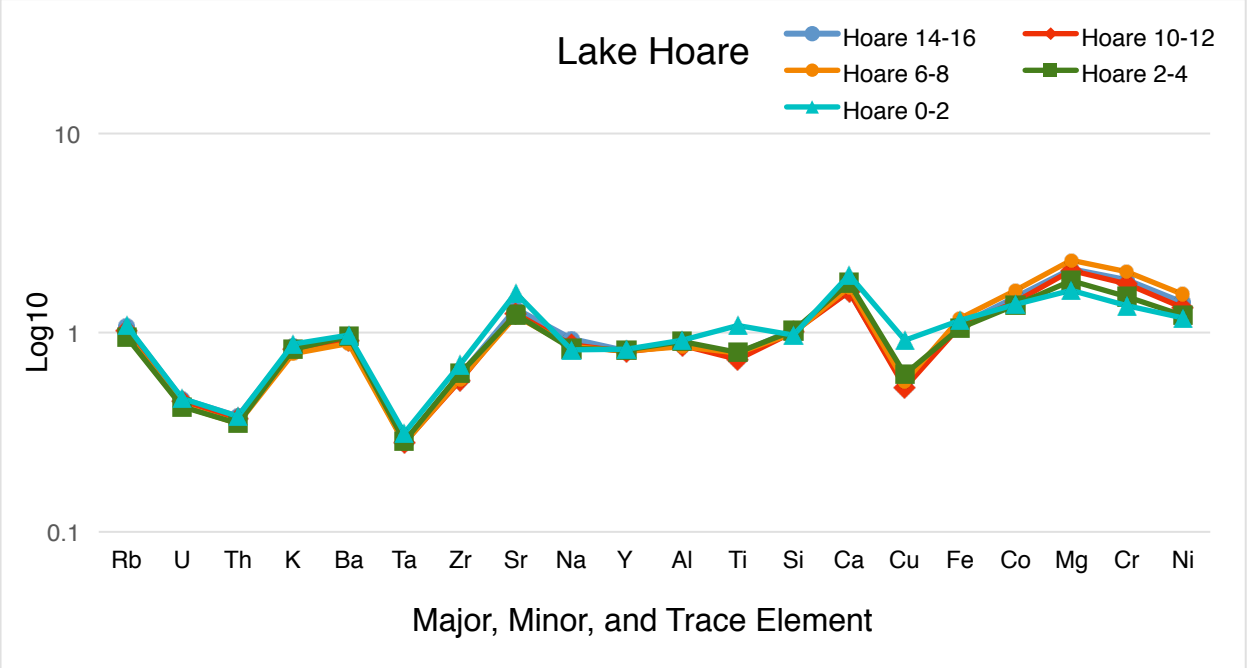

Figure 10. Spider diagram of major, minor, and trace elements of Lake Hoare sediments in order of crustal compatibility.

5. Discussion

The reason to compare the mineralogical and geochemical compositions of the Lake Hoare sediments and Pagoda samples was to determine the environmental conditions during their transport and deposition. The idea behind this work is to address the hypothesis: the similar physical environments in Antarctica over the span of at least 250 million years as reflected in the geochemical weathering status of the samples. The results suggest that there was more extensive chemical weathering resulting in a higher degree of alteration in the Pagoda samples compared to the modern Lake Hoare sediments. Both the mineralogical and the geochemical data support this idea. These results suggest that the climate during the Permian where the Pagoda samples were deposited was wetter than present times.

5.1 Mineralogy.

The sequence and thus extent of chemical weathering was determined by comparing the mineral assemblages of the modern sediments to the Pagoda samples. Quartz composed a large fraction of both the Pagoda samples and Lake Hoare sediments due to its lower temperature of crystallization that make quartz more stable at surface temperatures and pressures compared to other minerals (Ritter et al., 2011). The Pagoda samples contained primary minerals such as quartz and feldspar but also measurable amounts of clay minerals and secondary phyllosilicates that are assumed to be chemical weathering products. These clays are produced by the interaction of primary igneous alluminosilicate minerals with water and atmosphere CO_2 (to produce H_2CO_3). A generic chemical weathering reaction for a primary aluminosilicate mineral is as follows:

$$\text{Primary Mineral} + H_2O + CO_2 \rightarrow \text{Clay Mineral} + HCO^-_3 + H_4SiO_4 + \text{Dissolved Cations}$$

The Lake Hoare sediments contain stable mineral constituents such as quartz and felspar and a set of the least stable mineral constituents such as pyroxene and amphibole; there were no clay minerals measured by XRD. Presence of these minerals listed in Table 2 strongly suggests that the materials in the Pagoda samples have undergone more extensive chemical weathering.

5.2 Geochemistry.

5.2.1 CIA.

The CIA of the Lake Hoare sediments ranges between 53.8 and 54.9, falling into the category of little to no chemical alteration (Nesbitt and Young, 1982). Overall, these results reflect immature sediments that have not undergone much chemical weathering. These values are slightly higher than those observed in stream sediments throughout Taylor Valley (i.e. mean of 45.0) (Dowling et al. personal communicaiton). The Pagoda samples range from 66.1 to 72.3, categorizing them as highly altered material, suggesting abundant secondary weathering products such as clay minerals. Low CIAs reflect little to no chemical weathering, with primary minerals ~50 or less, and granites ranging from 45 to 55 (Nesbitt and Young, 1982).

5.2.2 Spider Diagrams.

The spider diagrams provide further support of the CIA calculations by pinpointing the depletion or enrichment of individual elemental constituents of each sample relative to the upper continental crust. The Pagoda samples show significant depletion of sodium and calcium, two of the most soluble of the major rock forming elements. Potassium, strontium, and other indicators of chemical weathering also show a slight depletion in most samples (Figure 9) while also showing a wide range of enrichments, thereby demonstrating little or no loss. The relative enrichment of potassium is perhaps explained by the mineralogy data given above, in that these samples contain detectable amounts of K-feldspar (orthoclase), muscovite, and biotite. The large

amounts of these un-weathered minerals in the Pagoda samples explain the relative enrichments in the geochemical data. Interestingly rubidium, uranium, and barium also usually depleted during moderate to severe chemical weathering usually show enrichments in these sediments. In general, more immobile elements like thorium, lead, hafnium, and most of the rare earth elements show no difference in enrichments relative to average upper continental crust. On the other hand, the Lake Hoare spider diagrams show little to no depletion of sodium, and in most cases, show enrichments in calcium (Figure 10). In addition, often very mobile elements such as rubidium, potassium, barium, and strontium show concentrations close to the average crustal values, and little to no weathering loss. The Lake Hoare sediments are depleted in uranium and thorium but enriched in magnesium, cobalt, nickel, and chromium reflecting the input of a higher portion of mafic provenance sediments (Dowling et al. in review). All this analysis assumes upper continental crust composition and must be taken with some reservation. Large variations, such as the loss of calcium and sodium in the Pagoda samples strongly indicate a more rigorous interaction of these sediments with water and a significant loss of the two most soluble major elements.

5.3 Integration of Mineralogical and Geochemical Data.

In general, there is a great agreement between both sets of data for both sample sets. The abundance of mineral weathering products and the CIAs, plus the evidence from the spider diagrams of loss of calcium and sodium from the Pagoda samples suggest that there was enough layered water present in the environment to alter the initial granitic derived sediments. This interpretation is supplemented by the sedimentological and paleontological work of Isbell et al. (2001). These authors suggested that the Pagoda Formation lacustrine sediments were transported and deposited under more temperate or at least warm-based glacier ice conditions,

prior to a major ice advance. Thus, the Pagoda sediments represent ice-marginal conditions, unlike today in the regions around the Transantarctic Mountains, where no sub-glacial out flow is known to exist currently (Fountain et al., 1999). In addition, the Isbell et al. (2001) work showed both the presence of wood fragments and thin fossils suggesting at least periods of optimal biological activity during periods of Pagoda Formation depositions in the Permian. The mineral and geochemistry of the modern Lake Hoare sediments clearly reflect the lack of liquid water throughout most of the year and the scant periods of input of sediments into the lake basin. In addition, most of the sediment introduced to Lake Hoare is through aeolian input to its surface ice which later melts through into the lake itself. The mineralogy dominated by primary minerals including higher weatherable ones such as augite and enstatite plus the low abundance of clay, and the enrichment of calcium and sodium suggest that chemical weathering is a minor consequence in this environment.

6. Conclusions.

- Both mineralogical and geochemical data suggest that the periglacial lake environment of the Pagoda Formation was very different from that of modern periglacial lakes such as modern Lake Hoare in the McMurdo Dry Valleys. During the Permian, the climate was wetter and hence warmer with more extensive chemical weathering taking place.

- The mineralogical data clearly show an abundance of both difficult to weather primary minerals, quartz and K-feldspar, as well as chemical weathering products (i.e., clay minerals such as illite, chlorite, and kaolinite) in the Pagoda samples. Lake Hoare mineralogy is dominated by igneous primary minerals, including ones that should weather early on, and few measurable clay minerals

- The Pagoda Formation has high chemical indices of alteration (CIA), while Lake Hoare sediments have CIA similar to unweathered igneous rocks.

- Major, minor, and trace element data normalized to average upper continental crust values indicate a loss of soluble calcium and sodium from the Pagoda samples, and little depletion from the Lake Hoare sediments. However, some soluble elements usually seen depleted under moderate weathering conditions, such as rubidium, potassium, barium, and uranium are not depleted in the Pagoda samples. The Lake Hoare sediments show little to no depletion, and in some cases enrichments in the most soluble elements, again, suggesting little to no chemical weathering. Some care must be taken interpreting these data. Provenance of the sediment has influence in these types of plots.

- The data presented here strongly support the interpretation of Isbell et al., (2001) concerning the climatic conditions during the transport and deposition of the Permian Pagoda Formation.

7. Recommendations for Future Work.

Further sample preparation must be conducted to determine the clay mineral compositions of the Pagoda samples. According to Brindley (1952), understanding d-spacings of certain clay minerals, heat treatments, dilution using HCL, and swelling methods using glycerol or ethanol glycol are effective techniques to distinguish certain clay compositions. The clay minerals from the Pagoda samples are the most weathered, and hence record the geological processes that occurred during the time of deposition at surface conditions. Temperature and therefore surface hydrology can be inferred from oxygen isotope ratios of the Pagoda Formation clays to more accurately infer paleoclimatic conditions of the Transantarctic Mountains during the Permian.

Outcrops of underlying Ordovician to Proterozoic aged granite basement rock could be analyzed to gauge their geochemistry to compare how relatively weathered the Pagoda Formation samples are.

REFERENCES CITED.

Allen P. P., Hewitt R., Maciej O. K., Doran P. T. (2015) Sediment transport dynamics on an ice-covered lake: the 'floating' boulders of Lake Hoare, Antarctica. *Antarctic Science*. **27 (2)**, 173-184.

Brindley G. W. (1952) Identification of Clay Minerals by X-ray Diffraction Analysis. *Clays and Clay Minerals.* Clay Mineral Society. **(1)**. pp. 119-129.

Doran P. T., Priscu J. C., Lyons W. B., Walsh J. E., Fountain A. G., McKnight D. M., Parsons A. N. (2002) Antarctic climate cooling and terrestrial ecosystem response. *Nature*. **415 (6871**), 517–520.

Faure G., Mensing T. M. (2010) *The Transantarctic Mountains: Rocks, Ice, Meteorites and Water.* Springer Science and Business Media, New York.

Fountain A.G., Thomas H. N., Monaghan A., Basagic H. J., and Bromwich D. (2010) Snow in the McMurdeo Dry Valleys, Antarctica. *International Journal of Climatology.* **(30)**, 633-642.

Isbell J. L., Miller M. F., Babcock L. E. (2001) Ice-marginal environment and ecosystem prior to initial advance of late Paleozoic ice sheet in the Mount Butters area of the Transantarctic Mountains, Antarctica. *Sedimentology*. **48**, 953-970.

Lindsay J. F. (1970) Institute of Polar Studies, Ohio State University, Columbus, Ohio. *Depositional Environment of Paleozoic Glacial Rocks in the Central Transantarctic Mountains*.

Lyons W. B., Fountain A., Doran P., Priscu J., Neumann K., and Welch K.A. (2000) Importance of landscape position and legacy: the evolution of the lakes in Taylor Valley, Antarctica. *Freshwater Biology*. **43(3)**, 355-367.

Lopez-Gamundi O. R. and Buatois L. A. (2010) Introduction: Late Paleozoic glacial events and postglacial transgressions in Gondwana. *Geological Society of America Special Papers.* **468**, v-viii.

Nesbitt, H. W and G. M. Young (1982) Early Proterozoic Climates and Plate Motions Inferred from Major Element Chemistry of Lutites. *Nature* **299**, 715-717.

Ritter D. F., Kochel C. R., Miller, Jerry R. (2011) *Process Geomorphology* (5th ed.) Waveland Press, Inc., Long Grove, Illinois.

Rudnick R. L. and Gao S. (2003) Composition of the continental crust. *Elsevier,* Amsterdam.

APPENDIX.

Appendix A.

Table A. Lake Hoare sediments (0-16cm) quantitative major, minor, and trace elements provided by the School of Earth Sciences XRF facility.

Element	Concentration	LH 14-16	LH 10-12	LH 6-8	LH 2-4	LH 0-2
Al2O3	weight %	0.889	0.864	0.853	0.9	0.915
SiO2	weight %	1.03	1.01	0.997	1.02	0.974
Fe2O3	weight %	1.41	1.39	1.514	1.35	1.48
CaO	weight %	1.61	1.61	1.69	1.78	1.95
TiO2	weight %	0.786	0.735	0.792	0.795	1.08
MgO	weight %	2.081	2.04	2.31	1.82	1.63
MnO	weight %	0.99	0.977	1.07	0.947	0.997
K2O	weight %	0.852	0.826	0.785	0.828	0.873
Na2O	weight %	0.932	0.872	0.852	0.829	0.819
P2O5	weight %	0.789	0.718	0.736	0.791	1.07
U	ppm	0.463	0.454	0.428	0.425	0.466
Th	ppm	0.381	0.371	0.35	0.349	0.379
K	ppm	0.852	0.826	0.785	0.828	0.873
Ba	ppm	0.963	0.917	0.889	0.966	0.977
Nb	ppm	0.763	0.73	0.719	0.761	0.882
Rb	ppm	1.07	1.02	0.966	0.95	1.09
Ta	ppm	0.281	0.28	0.278	0.285	0.313
Zr	ppm	0.611	0.574	0.581	0.623	0.69
Sr	ppm	1.32	1.25	1.22	1.23	1.58
P	ppm	0.789	0.718	0.736	0.791	1.07
Na	ppm	0.932	0.872	0.852	0.829	0.819
Y	ppm	0.804	0.804	0.808	0.818	0.826
Al	ppm	0.889	0.864	0.853	0.901	0.915
Ti	ppm	0.786	0.735	0.792	0.795	1.08
Si	ppm	0.889	0.864	0.853	0.901	0.974
Ca	ppm	1.61	1.61	1.69	1.78	1.95
Cu	ppm	0.547	0.528	0.567	0.62	0.914
Fe	ppm	1.41	1.39	1.51	1.354	1.49
Mn	ppm	0.99	0.977	1.07	0.947	0.997
V	ppm	1.17	1.15	1.29	1.14	1.15
Co	ppm	1.51	1.43	1.63	1.37	1.39
Mg	ppm	2.08	2.04	2.31	1.82	1.63
Zn	ppm	0.967	1.04	1.12	1.34	2.92
Cr	ppm	1.83	1.75	2.02	1.52	1.36

Ni	ppm	1.41	1.34	1.56	1.22	1.19

Appendix B.

Table B. Pagoda samples quantitative major, minor, and trace elements provided by SGS Mineral Services.

Element	Concentrations	Pagoda 1	Pagoda 2	Pagoda 3	Pagoda 4
	Weight (Kg)	0.006	0.007	0.011	0.008
SiO2	%	68.7	72.2	53.3	59
Al2O3	%	12.7	12	19.4	19.2
Fe2O3	%	7	4.73	11.3	6.36
MgO	%	2.89	2.07	3.24	2.92
CaO	%	0.89	0.79	1.72	0.59
K2O	%	3.03	3.26	6.1	6.2
Na2O	%	1.02	2.1	0.61	0.56
TiO2	%	0.53	0.47	0.92	0.91
MnO	%	0.11	0.13	0.12	0.09
P2O5	%	0.04	0.07	0.07	0.08
Cr2O3	%	0.03	<0.01	0.02	0.01
V2O5	%	<0.01	0.05	0.02	0.02
Al	%	6.75	6.27	10.2	10.3
Ba	%	1262	1158	1686	1495
Be	%	<5	<5	<5	<5
Ca	%	0.6	0.5	1.1	0.4
Cr	ppm	163	102	168	138
Cu	ppm	10	22	23	57
Fe	%	4.83	3.26	7.79	4.41
K	%	2.4	2.5	4.8	4.9
Li	ppm	56	38	94	72
Mg	%	1.61	1.16	1.85	1.67
Mn	ppm	794	929	885	662
Ni	ppm	49	34	208	59
P	%	0.01	0.03	0.03	0.03
Sc	ppm	8	7	21	18
Si	%	29.2	>30	24.8	27.1
Sr	ppm	248	222	311	255
Ti	%	0.29	0.26	0.5	0.51
V	ppm	55	235	82	137
Zn	ppm	118	75	104	109
Ag	ppm	<1	<1	<1	<1

As	ppm	<5	<5	<5	<5
Bi	ppm	0.1	0.4	0.1	0.6
Cd	ppm	<0.2	0.2	<0.2	<0.2
Ce	ppm	78.2	98	161	102
Co	ppm	24.1	14.3	15.1	19.2
Cs	ppm	5.9	3.7	25	16.6
Dy	ppm	5.33	8.99	7.28	6.53
Er	ppm	3.17	4.9	4.37	3.51
Eu	ppm	1.19	1.93	1.38	1.63
Ga	ppm	16	15	27	26
Gd	ppm	4.71	8.44	7.63	7.33
Ge	ppm	2	2	2	2
Hf	ppm	6	9	5	6
Ho	ppm	0.99	1.61	1.35	1.15
In	ppm	<0.2	<0.2	<0.2	<0.2
La	ppm	40	49.8	63.7	52
Lu	ppm	0.43	0.69	0.67	0.62
Mo	ppm	<2	3	<2	<2
Nb	ppm	9	9	20	18
Nd	ppm	32.2	46.3	53.3	47.4
Pb	ppm	40	63	31	40
Pr	ppm	8.62	11.7	14.1	12.3
Rb	ppm	118	153	300	266
Sb	ppm	0.3	0.1	1.9	0.5
Sm	ppm	5.7	9.6	10	9.6
Sn	ppm	3	2	6	5
Ta	ppm	0.6	0.6	1.4	1.3
Tb	ppm	0.73	1.37	1.1	1.02
Th	ppm	11.9	12.3	23.3	26.5
Tl	ppm	0.5	0.7	1.7	1.2
Tm	ppm	0.51	0.69	0.68	0.56
U	ppm	4.17	4.25	1.97	3.27
W	ppm	2	<1	3	4
Y	ppm	30.1	47.7	37.7	31.8
Yb	ppm	3.4	4.6	4.7	3.8
Zr	ppm	213	308	179	217

Appendix C.

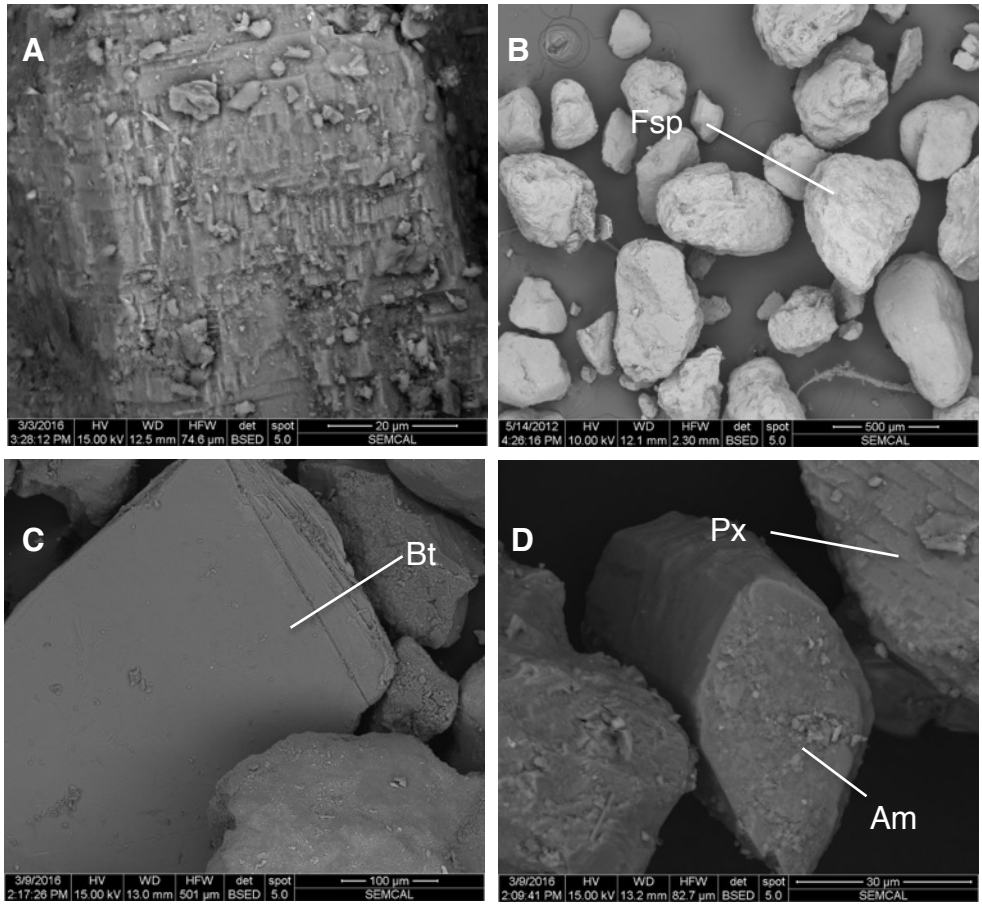

Figure C. SEM images of Lake Hoare sediments. A). Pyroxene exhibiting 90° cleavage and alteration. B). Sub-rounded feldspars with characteristic textured surfaces. C). Biotite grain exhibiting lamination. D). Amphibole with faint remnants of 60°-120° cleavage and pyroxene with striated surface.